Acta Cryst. (1964). **17**, 805

The Effects of Simultaneous Reflections on Single-Crystal Neutron Diffraction Intensities*

BY R. M. MOON† AND C. G. SHULL

Department of Physics, Massachusetts Institute of Technology, Cambridge, Mass., U.S.A.

(*Received* 8 *July* 1963)

The intensity changes produced in single-crystal diffraction reflections when one or more secondary reflections occur simultaneously are discussed both theoretically and experimentally. The theory is an extension of the usual treatment of secondary extinction, based on the mosaic crystal model. An approximate solution, valid in the thin crystal limit, is in good agreement with neutron diffraction experiments on single crystals of iron. Both theory and experiment demonstrate the importance of sample geometry on the magnitude and sign of the simultaneous reflection effects. The effects may be minimized by controlling the sample geometry in addition to the usual precautions taken to reduce secondary extinction.

Introduction

The interpretation of the intensity found in a single-crystal diffraction reflection is based on the assumption that only one Bragg reflection is occurring. However, it has long been known that the simultaneous occurrence of a second reflection is not uncommon and that the presence of a second reflection modifies the intensity of the first (primary) reflection. In accurate intensity measurements, this effect is as important as secondary extinction, yet it has received scant attention in the literature.

The simplest case of one secondary reflection is illustrated in Fig. 1. Point C is the center of the Ewald sphere of reflection which passes through the three reciprocal lattice points 0, 1 and 2. The directions of the incident, primary and secondary beams are given by unit vectors $\mathbf{S}_0$, $\mathbf{S}_1$ and $\mathbf{S}_2$. Instead of the customary Miller indices, it is convenient to designate reflection processes by two subscripts which describe the direction of the incident and reflected beam. Thus, the reciprocal lattice vector $\mathbf{H}_{12}$ is associated with a reflection from the direction $\mathbf{S}_1$ to the direction $\mathbf{S}_2$. It is important to realize that each of the beams can be reflected into each of the other two directions, so that when three lattice points are on the sphere, there are six reflection processes to consider.

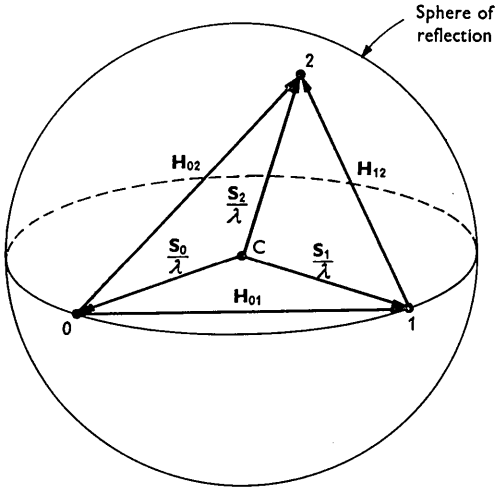

Fig. 1. Geometric representation of simultaneous reflections in the reciprocal lattice. Points 0, 1 and 2 lie on the sphere of reflection. The unit vectors $\mathbf{S}_0$, $\mathbf{S}_1$ and $\mathbf{S}_2$ define the direction of the incident, primary and secondary beams.

The first reported observation of the influence of simultaneous X-ray reflections concerned the effect called 'aufhellung' (Wagner, 1920) which corresponds to a diminution of the primary intensity. There are two processes constributing to this decrease: the reflection 0→2 removes power from the incident beam, thereby decreasing the power available for transfer in the 0→1 reflection; and the process 1→2 directly removes power from the primary reflected beam. These effects are opposed by the process 0→2→1 which adds power to the primary beam. The increase in primary power, called 'umweganregung', was first observed for X-rays by Renninger (1937), who made the first thorough experimental study of the simultaneous reflection effects. His experiment consisted in positioning the crystal and detector on a diffraction peak, then rotating the crystal about the scattering vector. In Fig. 1, the crystal is rotated in azimuth about the reciprocal lattice vector $\mathbf{H}_{01}$ and an intensity change in the primary beam is observed as point 2 passes through the sphere of reflection. His work is principally remembered for the large positive intensity variations found in the forbidden diamond (222) reflection, but it should be noted that he found both positive and negative intensity fluctuations of 10 to

* This research was supported by a grant from the National Science Foundation.

† Lincoln Staff Associate, now at Oak Ridge National Laboratory, Oak Ridge, Tennessee.

20 per cent in regular reflections of normal intensity, both in diamond and rocksalt.

Recently, many investigators (Hay, 1959; Spencer & Smith, 1959; O'Connor & Sosnowski, 1961; Duggal, Rao, Thapar & Singh, 1961; Schermer, 1961) have observed simultaneous reflection effects when analyzing the thermal neutron spectrum from a reactor by means of a crystal monochromator. In this, rapid changes in the crystal reflectivity are encountered as the scattered neutron energy is varied with scattering angle. When the monochromatic beam is used in an experiment measuring the transmission of a sample as a function of neutron energy, these rapid changes in the reflectivity of the monochromating crystal can look deceptively similar to a cross section resonance in the transmission sample. The present paper does not concern itself directly with the energy-dependent reflectivity, but rather, it will deal with the allied intensity problem in single-crystal diffraction experiments using nearly monochromatic radiation. Recent observations on monochromatic neutron intensity effects have been reported by Borgonovi & Caglioti (1962).

The simultaneous reflection problem separates naturally in two parts: determining the crystal orientation at which simultaneous reflections occur, and determining the intensity effect in a given primary reflection due to one or more secondary reflections. The orientation problem has been discussed elsewhere (Alexander, Fraenkel & Kalman, 1957; Cole, Chambers & Dunn, 1962), but the intensity problem has not been adequately treated. Mayer (1928) attempted to explain the 'aufhellung' effect in terms of Ewald's dynamical theory of X-ray diffraction. Renninger (1937) presented some helpful semi-quantitative arguments, but his treatment fell short of providing useful quantitative relationships. O'Connor & Sosnowski (1961) presented an approximate theory which agreed well with their observations using a neutron crystal spectrometer, but they omitted from the theory any mechanism which can result in 'Umweganregung'. Schermer (1961) has considered the formal solution of the intensity problem and worked out solutions in several cases of practical interest.

In the next section we present an approximate theory of the simultaneous reflection intensity problem for neutron diffraction which is valid in the limit of low secondary extinction. This is followed by a description of neutron diffraction experiments on iron single crystals which serve to check the theoretical conclusions. Preliminary reports on this work have been presented previously (Moon and Shull, 1961; Guentert, Moon, Shull & Bekebrede, 1961; Shull, 1962).

Theoretical calculation of intensity effects

We assume a well collimated, nearly monochromatic beam of neutrons is incident on a crystal such that Bragg reflection occurs from a set of primary reflecting planes. We wish to calculate the change in the power of this primary reflected beam when the azimuth angle is adjusted so that a second Bragg reflection is possible. The treatment is an extension of theory of secondary extinction based on the mosaic crystal model, as given, for example, by Bacon & Lowde (1948). Primary extinction is assumed to be negligible. It is also assumed that the orientation problem has been solved so that direction and indices of all the reflected beams are known.

The angular width associated with the incident beam collimation and wavelength spread is assumed to be much larger than the width of a perfect crystal reflection curve, but is much smaller than the width of the mosaic distribution. Under these conditions the reflected power at a particular angular setting of the crystal is interpreted as the integrated reflection produced by that portion of the mosaic distribution which is properly oriented.

An exchange of power from beam i to beam j is described in terms of a linear reflection coefficient r_{ij}, where

$$r_{ij}=Q_{ij}W(\Delta\theta_{ij})\,. \tag{1}$$

Q_{ij} is a well known crystallographic function equal to the integrated reflectivity per unit volume of a small crystallite and $W(\Delta\theta_{ij})$ is the mosaic distribution function. Note that $r_{ij}=r_{ji}$. A discussion of the proper evaluation of these reflection coefficients will be given later.

We consider a crystal in the shape of a flat plate which is large compared with the incident beam cross section. The following differential equations describe the change in power in the various beams as they traverse a crystal layer of thickness dx at depth x below the surface:

$$\frac{dP_0}{dx}=-\frac{P_0}{\gamma_0}(\mu+r_{01}+\sum_i r_{0i})+\frac{P_1}{\gamma_1}r_{10}+\sum_i\frac{P_i}{\gamma_i}r_{i0}\,, \tag{2}$$

$$\pm\frac{dP_1}{dx}=\frac{P_0}{\gamma_0}r_{01}-\frac{P_1}{\gamma_1}(\mu+r_{10}+\sum_i r_{1i})+\sum_i\frac{P_i}{\gamma_i}r_{i1}\,, \tag{3}$$

$$\pm\frac{dP_i}{dx}=\frac{P_0}{\gamma_0}r_{0i}+\frac{P_1}{\gamma_1}r_{1i}-\frac{P_i}{\gamma_i}(\mu+r_{i0}+r_{i1}+\sum_{j\neq i}r_{ij})+\sum_{j\neq i}\frac{P_i}{\gamma_j}r_{ji}\,, \tag{4}$$

where P_i is the power in beam i, γ_i is the magnitude of the direction cosine of beam i relative to the normal to the crystal surface, and μ is the linear absorption coefficient. The subscript 0 refers to the incident beam and 1 refers to the primary reflected beam. The summations extend over all secondary beams. The plus sign on the left side applies to the transmission case and the minus sign to the reflection case, as illustrated in Fig. 2.

The exact solution of these equations when several secondary beams are present is rather formidable and

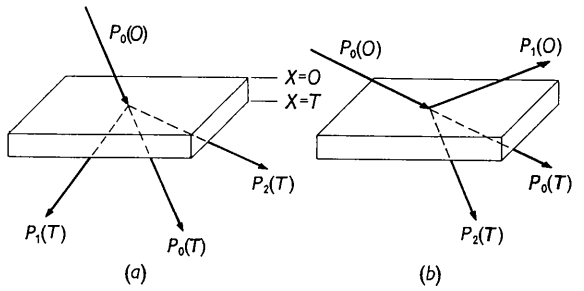

Fig. 2. Neutron beam passage through crystal plate: (*a*) Primary and secondary beams in transmission. (*b*) Primary beam in reflection; secondary beam in transmission.

probably not too useful owing to the multitude of special cases that are encountered in practice. Fortunately, a useful approximate solution can be obtained quite easily. We consider the case of low secondary extinction and low absorption, which is the usual case in experiments where quantitative use of intensity measurements is necessary. For the neutron case this implies that $r_i l_i \ll 1$ and $\mu l_i \ll 1$, where l_i is the path length of beam i in the crystal. If the crystal is of thickness T, then

$$l_i = T/\gamma_i \,. \tag{5}$$

For the case illustrated in Fig. 2(*a*), in which all secondary beams are of the transmission type, the boundary conditions at $x=0$ are $P_0=P_0(0)$ and $P_1=P_i=0$. We use a Taylor's series expansion of $P_1(x)$ about the point $x=0$, retaining terms up to the second order:

$$P_1(T) = P_1(0)+\left.\frac{dP_1}{dx}\right|_{x=0} T+\tfrac{1}{2}\left.\frac{d^2P_1}{dx^2}\right|_{x=0} T^2 \,. \tag{6}$$

Using the boundary conditions, the first term of equation (6) is zero and the second term is equal to $P_0(0)r_{01}l_0$. The third term is obtained by differentiating equation (3) and using the boundary conditions and equations (2), (3) and (4) to evaluate the resulting first derivatives. We obtain

$$\begin{aligned} P_1(T)/P_0(0) = {} & r_{01}l_0-\tfrac{1}{2}r_{01}l_0[\mu l_0+\mu l_1+r_{01}l_0+r_{10}l_1 \\ & +\sum_i(r_{0i}l_0+r_{1i}l_1)]+\tfrac{1}{2}\sum_i r_{0i}l_0r_{i1}l_i \,. \end{aligned} \tag{7}$$

If there are no secondary reflections, the corresponding solution is obtained by setting all r_{0i} equal to zero. The pure primary reflected power is thus,

$$P_1(T)/P_0(0) = r_{01}l_0[1-\tfrac{1}{2}(\mu l_0+\mu l_1+r_{01}l_0+r_{10}l_1)] \,. \tag{8}$$

The change in the primary reflection caused by the presence of the secondary beams is given by the difference between equations (7) and (8),

$$\Delta P_1(T)/P_0(0) = \tfrac{1}{2}\sum_i(-r_{01}l_0r_{0i}l_0-r_{01}l_0r_{1i}l_1+r_{0i}l_0r_{i1}l_i) \,. \tag{9}$$

Consider first the solution for the case of no secondary reflections, which is easy to solve exactly (See Bacon & Lowde, 1948 or Zachariasen, 1945). The exact solution for the symmetric transmisson case with one reflected beam is

$$P_1(T)/P_0(0) = \tfrac{1}{2}[1-\exp(-2r_{01}l_0)]\exp(-\mu l_0) \,. \tag{10}$$

It is easily shown that equation (10) reduces to equation (8) in the limit $r_{01}l_0 \ll 1$ and $\mu l_0 \ll 1$. Recall that $r_{01}=r_{10}$ and $l_0=l_1$ for symmetric transmission. It is more interesting to note that the exact solution for the symmetric reflection case also reduces to equation (8) even though the boundary conditions are different. This may be most easily seen from the zero absorption case, for which the exact solution for the symmetric reflection case is

$$P_1(T)/P_0(0) = r_{01}l_0/(1+r_{01}l_0) \,. \tag{11}$$

The fact that equation (8) is a good approximation in the low extinction limit for either the transmission or reflection cases illustrates an important property of the approximate solution when simultaneous reflections are present. It can be shown that equation (7) is valid up to terms of second order in the reflectivities regardless of the boundary conditions, provided that we are dealing with a flat plate sample. That is, the reflected beams can be of either transmission type or reflection type or any mixture thereof.

The effects of simultaneous reflections are conveniently discussed by examining equation (9). The two negative terms are similar to the usual secondary extinction correction and describe the effect called 'aufhellung'. The first term of equation (9) represents that portion of the power reflected from the incident beam into beam i, which would have been reflected into the primary beam in the absence of the secondary reflection. The second term accounts for the direct reduction of the primary beam by reflection into the various secondary beams. The third term accounts for 'umweganregung', the increase in the primary beam by reflections into this beam from all the secondary beams.

We turn now to an evaluation of the reflectivity coefficients, defined in equation (1). The familiar expressions for Q and the mosaic distribution function are valid when the crystal is rotated about an axis normal to the incident and reflected beams, as in the usual rocking curve experiment. This relationship will not be satisfied for the secondary reflections, so we desire general expressions for Q and the mosaic distribution, valid for rotation about an arbitrary axis. We assume the mosaic distribution to be of Gaussian form

$$W(\Delta\theta_{ij}) = [(2\pi)^{\frac{1}{2}}\eta]^{-1}\exp[-(\Delta\theta_{ij})^2/2\eta^2], \tag{12}$$

where $\Delta\theta_{ij}$ is the deviation in Bragg angle from the mean of the distribution. It can be shown that

$$\Delta\theta_{ij} = (\sin\psi\cos\chi\cos\xi/\sin 2\theta)_{ij}\Delta\varepsilon = K^{\varepsilon}_{ij}\Delta\varepsilon, \tag{13}$$

where $\Delta\varepsilon$ is a small change in angle about an arbitrary axis and the angles are defined in Fig. 3. The mosaic distribution may now be written in terms of the general rotation angle and renormalized to unity,

$$W(\Delta\varepsilon) = K^{\varepsilon}_{ij}[(2\pi)^{\frac{1}{2}}\eta]^{-1}\exp\left[-(K^{\varepsilon}_{ij}\Delta\varepsilon)^2/2\eta^2\right]. \quad (14)$$

Zachariasen (1945) has given an expression for Q for an arbitrary crystal rotation. In neutron terminology, his equation is

$$Q'_{ij} = \left(\frac{\lambda^3 N^2|F|^2}{\sin\psi\cos\chi\cos\xi}\right)_{ij} = \left(\frac{\lambda^3 N_2|F|^2}{\sin 2\theta}\right)_{ij}\frac{1}{K^{\varepsilon}_{ij}} = \frac{Q_{ij}}{K^{\varepsilon}_{ij}} \quad (15)$$

where λ is the wavelength, N is the number of unit cells per unit volume and F is the structure factor per unit cell. The quantity Q_{ij} is the Q associated with the integrated intensity in a normal crystal rotation experiment.

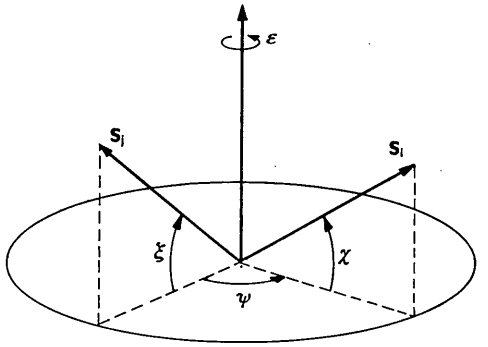

Fig. 3. Definition of angles involved in crystal reflectivity r_{ij} with crystal rotation about an arbitrary axis. The plane in which ψ_{ij} is measured is perpendicular to the rotation axis.

The complete reflectivity expression may then be written as

$$r_{ij} = Q_{ij}[(2\pi)^{\frac{1}{2}}\eta]^{-1}\exp\left[-(K^{\varepsilon}_{ij}\Delta\varepsilon)^2/2\eta^2\right]. \quad (16)$$

Three dimensionless ratios R_P, R_R and R_D which can be experimentally determined have been considered in attempting to provide a useful measure of the magnitude of the effects of simultaneous reflections. These are illustrated in Fig. 4. In the Renninger experiment, the Bragg angle is fixed at the center of the primary reflection peak and the crystal is rotated about the scattering vector. The quantity R_P is the maximum fractional change in the counting rate as the azimuthal angle is varied from the peak azimuthal angle φ_0 to an angle φ_A away from the simultaneous reflection peak. It is obtained from equations (9) and (16) by evaluating all the reflectivities at their peak value,

$$R_P = \Delta P_1(\theta_0,\varphi_0)/P_1(\theta_0,\varphi_A) = \tfrac{1}{2}\left[\frac{Q_{01}l_0}{(2\pi)^{\frac{1}{2}}\eta}\right]\sum_i\left[-\left(\frac{Q_{0i}}{Q_{01}}\right)-\left(\frac{Q_{1i}}{Q_{01}}\right)\left(\frac{l_1}{l_0}\right)+\left(\frac{Q_{0i}Q_{i1}}{Q^2_{01}}\right)\left(\frac{l_i}{l_0}\right)\right]. \quad (17)$$

In equations (17), (18) and (19), we take $P_1(\theta,\varphi_A) = r_{01}l_0$.

The quantity R_R is obtained experimentally by integrating the intensity above the base line in the Renninger experiment and dividing by the normal integrated intensity in the absence of any simultaneous reflections. It is evaluated theoretically by identifying ε in equation (16) with the azimuthal angle φ and substituting the appropriate reflectivities into equation (9). The primary reflectivity, r_{01}, is evaluated at its peak because the rotation is about the primary scattering vector, and the integrations carried out over the other reflectivities. We obtain

$$R_R = \int\Delta P_1(\theta_0,\varphi)d\varphi\Big/\int P_1(\theta,\varphi_A)d\theta = \tfrac{1}{2}\left[\frac{Q_{01}l_0}{(2\pi)^{\frac{1}{2}}\eta}\right]\sum_i\left[-\left(\frac{1}{K^{\varphi}_{0i}}\right)\left(\frac{Q_{0i}}{Q_{01}}\right)-\left(\frac{1}{K^{\varphi}_{1i}}\right)\left(\frac{Q_{1i}}{Q_{01}}\right)\left(\frac{l_1}{l_0}\right)+\left\{(K^{\varphi}_{0i})^2+(K^{\varphi}_{i1})^2\right\}^{-\frac{1}{2}}\left(\frac{Q_{0i}Q_{i1}}{Q^2_{01}}\right)\left(\frac{l_i}{l_0}\right)\right]. \quad (18)$$

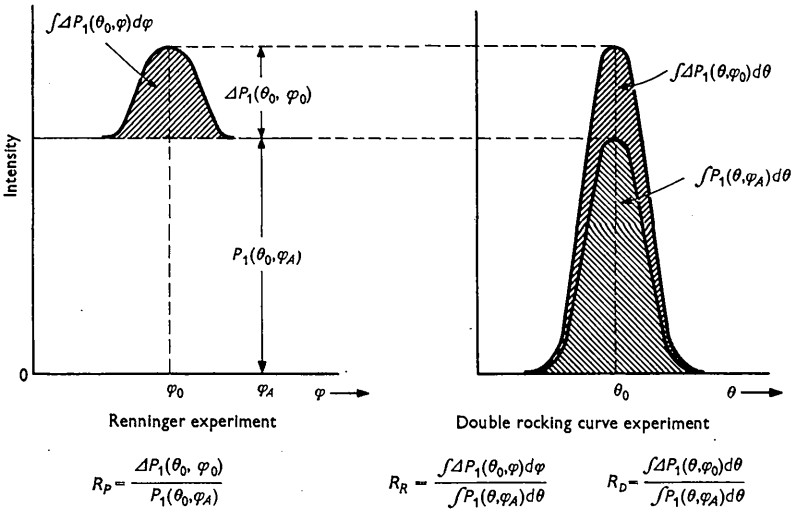

Fig. 4. Definition of ratios useful for quantitative evaluation of simultaneous reflection effects.

Finally, the ratio R_D is obtained by measuring two rocking curves in the normal manner, one with the azimuth fixed on a simultaneous reflection peak and one where no simultaneous reflections are present. The ratio is calculated by identifying ε in equation (16) with the Bragg angle θ, substituting into equation (9), and integrating over all the reflectivities. We obtain

$$\begin{aligned} R_D &= \int \Delta P_1(\theta,\varphi_0)d\theta / \int P_1(\theta,\varphi_A)d\theta \\ &= \tfrac{1}{2}\left[\frac{Q_{01}l_0}{(2\pi)^{\frac{1}{2}}\eta}\right] \sum_i \Big[-\{1+(K_{0i}^{\theta})^2\}^{-\frac{1}{2}} \left(\frac{Q_{0i}}{Q_{01}}\right) \\ &\quad -\{1+(K_{1i}^{\theta})^2\}^{-\frac{1}{2}} \left(\frac{Q_{1i}}{Q_{01}}\right)\left(\frac{l_1}{l_0}\right) \\ &\quad +\{(K_{0i}^{\theta})^2+(K_{i1}^{\theta})^2\}^{-\frac{1}{2}} \left(\frac{Q_{0i}Q_{i1}}{Q_{01}^2}\right)\left(\frac{l_i}{l_0}\right)\Big]. \end{aligned} \tag{19}$$

The ratios inside the summations in equations (17), (18) and (19) are frequently near unity, so that the size of the effect is determined by the factor $Q_{01}l_0/(2\pi)^{\frac{1}{2}}\eta$. This is the same factor as determines the size of the secondary extinction correction. We conclude that the effects of simultaneous reflections may be present in all experiments where secondary extinction is not negligible, and the magnitudes of the two effects are frequently about the same. If there is doubt whether secondary extinction is important in an experiment, the azimuthal sweep may be useful. If no intensity perturbations are observed, the evidence is strong for negligible secondary extinction.

There are important cases in which the simultaneous reflection effects are quite large even though secondary extinction may be small. Large fractional intensity changes can occur when the secondary reflectivities are large compared with the primary reflectivity,

$$\left(\frac{Q_{0i}}{Q_{01}}, \frac{Q_{1i}}{Q_{01}} \gg 1\right).$$

The extreme case is illustrated by Renninger's measurements on the diamond (222) reflection. In this case $Q_{01}=0$, so that only the positive term remains in equation (9).

If the Q ratios in equations (17), (18) and (19) are approximately equal to unity, then the factor l_i/l_0 is of decisive influence in determining the magnitude and sign of the simultaneous reflection effects. A long secondary beam path length can result in a large positive intensity change even though the secondary extinction effect is small. This is demonstrated in the experiments described in the next section.

Most of the above discussion applies to the X-ray case as well except that the path lengths are determined in general by absorption rather than by the crystal geometry.

Experimental studies

Experiments similar to those described by Renninger (1937) were performed on iron crystals with the single-crystal neutron spectrometer at the MIT Nuclear Reactor. The samples were mounted on a goniometer featuring a horizontal rotation axis and a device for adjusting the crystal orientation relative to the rotation axis. The final adjustment of the crystal orientation was made by sweeping the goniometer and neutron counter, in $\theta, 2\theta$ relationship, through the primary reflection peak at four different azimuthal angles separated by 90°. When the four peaks occurred at the same crystal θ angle, the primary scattering vector was parallel to the azimuthal rotation axis. The goniometer and counter were then fixed at the primary reflection peak and the crystal was slowly rotated in azimuth by means of a small electric motor.

Typical results are shown in Fig. 5 for an iron crystal in the form of a flat plate (6·3 × 5·8 × 0·6 mm). The mosaic width parameter, η, was found to be 0·40° by measuring the width of the rocking curve with a nearly perfect crystal of matched d spacing as the monochromator. The incident neutron beam was of large cross section, so that the entire sample was bathed in a beam of nearly uniform intensity. A rather long wavelength (1·57 Å) was used in the experiment so as to separate the secondary reflections in azimuthal angle. The indices above the peaks and dips correspond to reciprocal lattice points which lie on the sphere of reflection at that particular azimuth. The base line, representing the true (200) peak intensity, was not flat because the mosaic spread exhibited directional properties. The pattern had reflection symmetry about the 45° azimuth position. The two curves are for the same crystal, one with the primary beam in symmetric reflection and the other in symmetric transmission. The difference between the two curves clearly illustrates the decisive influence of the sample geometry on the characteristics of the observed pattern. Note that in the symmetric reflection case, the positive peaks all result from secondary reflections of the type $(1kl)$. For these cases, the direction of the secondary beam is in the plane of the crystal so that the associated path length is long. In equation (17), this means that the positive term is large by virtue of the large l_i/l_0 ratio. For the same secondary reflections in the symmetric transmission case, $l_i = l_0$, and we observe that the negative terms are dominant.

The experiments differed in several aspects from the assumptions made in the theory. In the theory the beam cross section was small compared with the crystal while the opposite was true in the experiments. Suitable average path lengths based on the crystal dimensions and the various beam directions were used in the comparison between theory and experiment. Secondly, the basic assumption that $r_{ij}l_i \ll 1$ was not very well satisfied for the cases where l_i was in the plane of the crystal. To improve the approximation, those third order terms in the Taylor's series expansion involving the long path length were included for the comparison calculation. This had the effect of providing an extinction correction for the secondary beam;

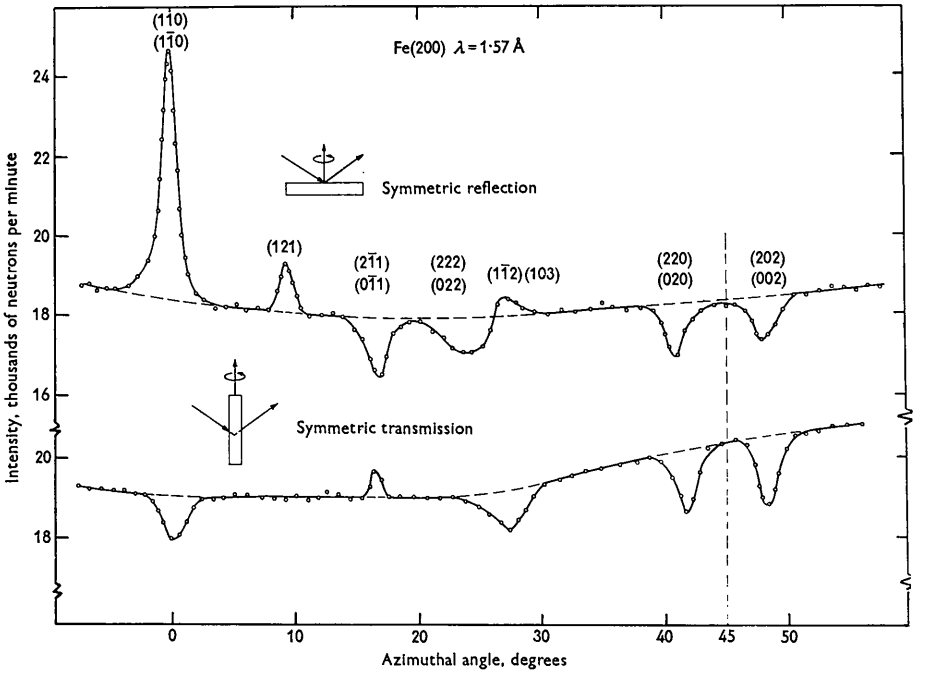

Fig. 5. Simultaneous reflection effects observed in the 200 reflection from iron as the crystal is rotated around the scattering vector. Pronounced differences are to be noted for the reflecting and transmitting crystals.

Table 1. *Comparison between calculated and observed intensity ratios*

Primary reflection: Fe(200), $\lambda = 1{\cdot}565$ Å

		Reflection case				Transmission case			
$(hkl)_{0i}$	φ	R_R Calc.	R_R Obs.	R_P Calc.	R_P Obs.	R_R Calc.	R_R Obs.	R_P Calc.	R_P Obs.
(110) (1$\bar{1}$0)	0°	+0·30	+0·36	+0·29	+0·28	−0·10	−0·10	−0·04	−0·05
(121)	8·6	+0·05	+0·05	+0·07	+0·03	−0·01	0·00	−0·01	0·00
(2$\bar{1}$1) (0$\bar{1}$1)	17·4	−0·14	−0·15	−0·07	−0·08	+0·01	+0·02	+0·05	+0·04
(222) (022)	21·6	−0·15	−0·16	−0·07	−0·06	−0·03	−0·02	+0·02	−0·01
(1$\bar{1}$2)	27·7	+0·05	+0·05	+0·07	+0·05	−0·06*	−0·07*	−0·04*	−0·04*
(103)	29·8	+0·05	+0·03	+0·07	+0·02				
(220) (020)	40·6	−0·13	−0·15	−0·07	−0·08	−0·11	−0·11	−0·06	−0·07

* The (1$\bar{1}$2) and (103) dips were not experimentally resolved in this case. The calculated numbers were added for the two cases.

the positive term in equation (9) was multiplied by a factor $[1-\frac{1}{3}(r_{i0}l_i+r_{il}l_i)]$. The theory also assumed that the instrumental broadening was very small compared with the mosaic spread. In the experiment, the instrumental broadening was smaller than the width due to the mosaic spread, but both were of the same order of magnitude. This disagreement between theory and experiment casts doubt on the validity of the peak ratio calculation (equation 17), but the integrated ratio (equation 18) should show better agreement with experiment. Of course, the mosaic distribution was not a true Gaussian and, as we have noted, it showed directional properties, so at best we can hope for only approximate agreement.

The comparison between theory and experiment is shown in Table 1. The experimental values in Table 1 are averages obtained in several runs. In most cases the spread in the experimental values was larger than the difference between the experimental average and the calculated number. The calculations contain one experimentally determined parameter, the factor $Q_{01}l_0/(2\pi)^{\frac{1}{2}}\eta$ which appears as a scale factor in equations (17) and (18). This can be obtained either by measuring the peak absolute reflectivity in the absence of any secondary reflections,

$$P_1(\theta_0,\varphi_A)/P_0 \simeq \left[\frac{Q_{01}l_0}{(2\pi)^{\frac{1}{2}}\eta}\right]\left[1-\frac{Q_{01}l_0}{(2\pi)^{\frac{1}{2}}\eta}\right] \qquad (20)$$

or by measuring η and the absolute integrated reflectivity,

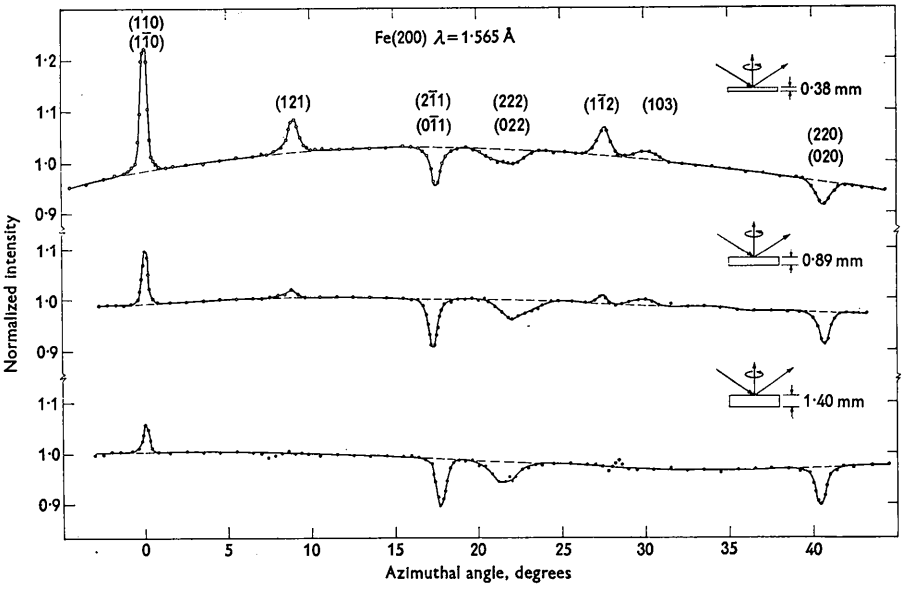

Fig. 6. Effect of sample thickness of the simultaneous reflection pattern. For the positive peaks, I_i/I_0 decreases as the thickness increases.

$$\int P_1(\theta,\varphi_A)d\theta/P_0 \cong Q_{01}l_0[1-Q_{01}l_0/(2\pi)^{\frac{1}{2}}\eta]\,. \quad (21)$$

A value of 0·0674 for $Q_{01}l_0/(2\pi)^{\frac{1}{2}}\eta$ was obtained for the symmetric reflection case by the first method and 0·0706 by the second method. The peak reflectivity value was used in the calculations since it is a direct measure of the experimental base line. The terms inside the summation in equations (17) and (18), which determine the direction and relative magnitude of the simultaneous reflection peaks, were calculated from the known reflection processes and the sample geometry.

Another illustration of the importance of sample geometry is contained in Fig. 6. Simultaneous reflection patterns were obtained for three samples, cut from the same crystal, and differing only in their thickness. With the primary beam in symmetric reflection, the positive peaks occur in cases where the secondary beam is in the plane of the crystal. As the crystal thickness is increased, these secondary path lengths remain the same, but the primary path length, l_0, increases. The ratio I_i/I_0 then decreases, and it follows from equation (17) that the positive peaks should decrease. The negative peaks should increase in magnitude, but much less dramatically. These expectations are fully confirmed by experiment. Quantitative comparison was not attempted for this experiment because the basic assumption of low secondary extinction was not satisfied.

A further confirmation of the importance of the secondary beam path length is contained in Fig. 7. The simultaneous reflections involved in this illustration are the same as for the large positive peak at 0° azimuth in Fig. 5. The two secondary beams are in the plane of the crystal as indicated in the figure. By

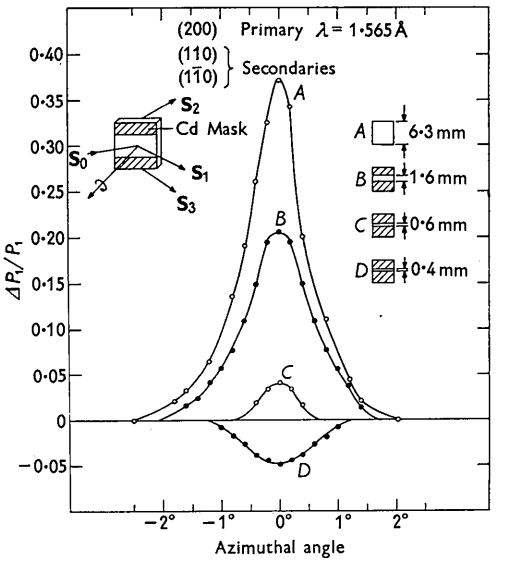

Fig. 7. Effect of sample cross-section on a simultaneous reflection peak. As the effective size of the sample is reduced, the ratio I_i/I_0 decreases.

covering part of the crystal with a cadmium mask, the path length of the secondary beam which is effective in returning intensity back to the primary reflection is reduced. The positive term inside the summation in equation (17) gets progressively smaller as more and more of the crystal is covered while the negative terms remain unaffected.

The theory contains some interesting predictions concerning the shape of the simultaneous reflection peaks as the azimuthal angle is varied. The negative

term in equation (9) contain only one Gaussian function because r_{01} is evaluated at its peak, while the positive term contains a product of two Gaussians. This means that the positive term is generally narrower than the negative terms. We conclude that peaks in which the positive terms is dominant should be narrower than the negative dips. Also, if all the assumptions in the theory are valid, the positive peaks should have negative wings since the negative contribution falls off slower with $\Delta\varphi$ than does the positive term. The same peak shape was predicted by Schermer (1961). This shape has not been observed for peaks resulting from a single secondary reflection, but it has been observed in one case where many secondary beams are present, some giving positive contributions and others negative. Based on a mosaic spread parameter $\eta=0{\cdot}4°$, the calculated width at half maximum of the positive peak at 0° in the symmetric reflection of Fig. 5 is 1·0°, while the dip at 0° in the transmission case should have a width of 2·2°. The observed values are 1·1° and 2·6°.

The experiments give some measure of confidence in using the equations of the preceding section to calculate the effects of simultaneous reflections. It should be emphasized that the theoretical assumptions are the same as contained in the theory for the low secondary extinction case. Since experiments are usually arranged to meet the requirements of low secondary extinction, the theory presented here should be generally applicable to the practical case.

Conclusions

The present investigation emphasizes the necessity of considering the presence of secondary reflections in accurate measurements of primary reflection intensities from single crystals. An assessment of the secondary perturbations can sometimes be made by studying the azimuthal rocking curves but, as Renninger pointed out, this is difficult at short wavelengths because of the increased frequency of the simultaneous reflections. Our calculations for the iron pattern show that in a 45° azimuthal sweep at $\lambda=1{\cdot}56$ Å there are seven peaks due to reflections occurring simultaneously with the 200 primary one while at 0·716 Å this number has increased to seventy eight.

As a general rule, the magnitude of the intensity perturbations is comparable to the intensity corrections that arise due to secondary extinction. Hence the extraneous intensity effects may be reduced by using small crystals with broad mosaic character. However, even when secondary extinction is quite small, large positive secondary effects can occur if the linear reflectivities in the $0 \rightarrow 2$ and $2 \rightarrow 1$ processes are large compared with the primary $0 \rightarrow 1$ process or if the secondary ray path length is long. The experimenter has some control over the latter event by selection of the crystal geometry. Clearly it is better to use a specimen crystal which is long in only one direction rather than a flat disk or square plate.

In any event, it is wise to precede accurate intensity measurements by an azimuthal sweep to assay the simultaneous reflection effects. If these effects cannot be avoided the formulae presented above should allow intensity corrections to be applied with about the same accuracy as is present in secondary extinction corrections.

We are pleased to acknowledge helpful discussions with O. J. Guentert and H. Cole. We are indebted to F. Ricci and W. C. Phillips for experimental help during the early stages of this work.

References

ALEXANDER, E., FRAENKEL, B. S. & KALMAN, Z. H. (1959). Tech. Report 1, contract AF 61(052)-222, Hebrew University, Jerusalem.

BACON, G. E. & LOWDE, R. D. (1948). *Acta Cryst.* **1**, 303.

BORGONOVI, G. & CAGLIOTI, G. (1962). *Nuovo Cim.* X, **24**, 1174.

COLE, H., CHAMBERS, F. W. & DUNN, H. M. (1962). *Acta Cryst.* **15**, 138.

DUGGAL, V. P., RAO, K. R., THAPAR, C. L. & SINGH, V. (1961). *Proc. Indian Acad. Sci.* **53**, 59.

GUENTERT, O. J., MOON, R. M., SHULL, C. G. & BEKEBREDE, W. R. (1961). Ann. Meeting Amer. Cryst. Assoc., 1961. Boulder, Colorado.

HAY, H. J. (1959). Atomic Energy Research Establishment, Report No. R 2982, Harwell, Berkshire, England.

MAYER, G. (1928). *Z. Kristallogr.* **66**, 585.

MOON, R. M. & SHULL, C. G. (1961). *Bull. Amer. Phys. Soc.* **6**, 261.

O'CONNOR, D. A. & SOSNOWSKI, J. (1961). *Acta Cryst.* **14**, 292.

RENNINGER, M. (1937). *Z. Phys.* **106**, 141.

SCHERMER, R. I. (1961). *Bull. Amer. Phys. Soc.* **6**, 261.

SHULL, C. G. (1962). *Lecture Notes on Neutron Crystal Spectrometry.* Kjeller, Norway: Institutt for Atomenergi.

SPENCER, R. R. & SMITH, J. R. (1959). *Bull. Amer. Phys. Soc.* **4**, 245.

WAGNER, R. (1920). *Phys. Z.* **21**, 632.

ZACHARIASEN, W. H. (1945). *Theory of X-ray Diffraction In Crystals*, pp. 106–161. New York: Wiley.